Shahrood University of Technology

Journal of Mining and Environment (JME)

Journal homepage: www.jme.shahroodut.ac.ir

Iranian Society of Mining Engineering (IRSME)

Grade Estimation Through the Gaussian Copulas: A Case Study

Babak Sohrabian[1]*, and Abdullah Erhan Tercan[2]

1. Associate Professor, Department of Mining Engineering, Faculty of Environment, Urmia University of Technology, Urmia, Iran
2. Professor, Department of Mining Engineering, Hacettepe University, Ankara, Turkey

Article Info

Received 5 March 2024
Received in Revised form 15 June 2024
Accepted 28 June 2024
Published online 28 June 2024

DOI: 10.22044/jme.2024.14287.2668

Keywords

Gaussian copula
Indicator kriging
Jackknife test
Ordinary kriging
Porphyry copper deposit

Abstract

Mineral Resources have commonly been estimated through the kriging method that assigns weights to the samples based on variogram distance to the estimation point without considering their values. More robust estimators such as spatial copulas are promising tools because they consider both distance and sample values in determining weights. The purpose of this study is to demonstrate the effectiveness of the Gaussian copulas (GC) by estimating the copper grade values in the Sungun porphyry copper deposit located in Iran. Performance of the method was compared to ordinary kriging (OK) and indicator kriging (IK) by running the Jackknife test of cross-validation. The metrics used in measuring performance of the methods are global accuracy and precision of the distribution of the estimates, error statistics, and variability for globally accurate and precise estimates. The case study shows advantages of GC over OK and IK by producing globally accurate and precise estimates with acceptable error statistics and variability.

1. Introduction

Evaluation of mineral deposits is implemented based on a limited number of boreholes, that reveal a small portion of these deposits. Therefore, in the remaining parts, grade values should be estimated based on available samples using robust estimators. Ordinary kriging (OK) and indicator kriging (IK) are traditional methods used in estimation [1-5]. These methods are based on a weighted moving average technique, which assigns weights to local data regarding their distance from the estimation point and their spatial configuration; but sample values do not have any impact on the weights [6-7]. Moreover, ordinary kriging cannot calculate confidence intervals for the estimates, intrinsically. This method gives symmetric confidence intervals through the application of multi-Gaussianity assumption and, for reaching reasonable outcomes, it needs prior transformation of data into normal distribution. Therefore, IK with the ability of deriving conditional cumulative distribution functions was developed to tackle this drawback of the OK. However, smoothing problem of IK is greater than OK and it gives estimates that are gathered around the mean value of variable under study. Another issue about the IK is associated with ranking order problem such that this method may give unacceptable probability of occurrence for some thresholds [8-9] and it is needed to carry out posterior correction [10-11]. Because of the above-mentioned issues, application of new methods that tackle these problems and give reasonable estimates would be helpful.

In the literature, the Gaussian copulas (GC) are proposed as alternatives to kriging in the estimation of spatially dependent variables due to their ability to use data configuration as well as sample values in assigning weights to them [12-15]. Similar to the IK, the Gaussian copulas allow to derive conditional cumulative distribution at unknown locations and, consequently, calculate confidence intervals for the estimates [16-19]. However, in contrast to the IK, the copula approach does not

Corresponding author: babak_sohrabian@uut.ac.ir (B. Sohrabian)

have order relation violation. Moreover, spatial copula provides more accurate and precise estimates than kriging.

In this study, the aim is to show the effectiveness of the GC by applying it to a data set obtained from the Sungun porphyry copper deposit, Iran. The GS is compared to OK and IK through running a Jackknife test and also estimating the whole deposit. In most studies such as Musafer et al. [20], Addo et al. [21] Sohrabian et al. [22] and Bárdossy and Hörning [23], different kinds of copulas, which are non-parametric estimators, have only been compared to OK, which is a linear estimator. The first novelty of the current study is evaluating the GC against a non-parametric method such as IK. The second novelty is associated with the application of more rigorous statistical tests such as global accuracy and precision in assessing the results.

The paper is structured as follows. Section two provides a brief theory on spatial estimation by GC. Third section gives a case study including a Jackknife test of cross-validation and grade estimation on a 3D regular mesh. The GC results are compared to those of OK and IK. Last section presents the conclusions.

2. Methods

This section begins giving a brief theory on the Gaussian copulas, which are symmetric practical tools in delineating dependence structure of variables. In its traditional form, the Gaussian copulas do not have distance parameter in their algorithm. Therefore, for geostatistical application, it is parameterized by distance and correlogram analysis in studies such as Bardossy [12], Bardossy and Li [13], and Atalay and Tercan [15]. The remaining part of this section gives steps of estimation through the Gaussian. Then, ordinary and indicator kriging methods are presented and some performance criteria are presented for evaluation of the estimation methods.

2.1. Gaussian Copula

Copula, C, is a function that delineates the dependence structure of variables as follows:

$$C: [0,1]^n \rightarrow [0,1] \quad (1)$$

If one of the variables becomes zero, the copula takes zero value as well. According to Sklar [24], any n-variate distribution $F(Z_1, \dots, Z_n)$ can be represented by its margins, $F_{Z_i}(Z_i)$, and n-dimensional copula, C:

$$F(Z_1, \dots, Z_n) = C\left(F_{Z_1}(Z_1), \dots, F_{Z_n}(Z_n)\right) \quad (2)$$

The copula method assumes that variables under study are second-order stationary with identical margins over the study area [25]. In this method, by transforming the continuous variables into standard uniform distributions through $U_i = F_{Z_i}(Z_i)$, the copula becomes a unique function which does not depend on the marginal distributions anymore and can be expressed based on the mutual dependence structure:

$$C(Z) = F(F_{Z_1}^{-1}(Z_1), \dots, F_{Z_n}^{-1}(Z_n)) \quad (3)$$

The inverse function of ith marginal distribution is denoted by $F_{Z_i}^{-1}(Z_i), i = 1, \dots, n$. The density of copula, c, can be defined as partial derivatives as follows:

$$c(u_1, \dots, u_n) = \frac{\partial^n C(u_1, \dots, u_n)}{\partial u_1 \dots \partial u_n} \quad (4)$$

in Equation (4), $\frac{\partial^n}{\partial u_n}$ is the partial derivatives of copula with respect to the nth marginal distribution. Then, the conditional copula takes the following form:

$$C(u_1 \mid U_2 = u_2, \dots, U_n = u_n) = \frac{\partial^{n-1} C(u_1, \dots, u_n)}{\partial u_2 \dots \partial u_n} \times \frac{1}{c(u_2, \dots, u_n)} \quad (5)$$

For a multivariate Gaussian case with correlation matrix, R, Equation (3) becomes:

$$C_R(Z) = \varphi(\varphi^{-1}(Z_1), \dots, \varphi^{-1}(Z_n)) \quad (6)$$

where, φ and φ^{-1} are respectively multivariate standard normal distribution and its inverse function. The multivariate Gaussian density function, $c_R(.)$, can be calculated as follows:

$$c_R(Z) = \frac{1}{\sqrt{|R|}} exp\left\{-\frac{1}{2}\begin{bmatrix}\Phi^{-1}(Z_1)\\ \vdots \\ \Phi^{-1}(Z_n)\end{bmatrix}^T (R^{-1} - I)\begin{bmatrix}\Phi^{-1}(Z_1)\\ \vdots \\ \Phi^{-1}(Z_n)\end{bmatrix}\right\} \quad (7)$$

where the determinant of correlation matrix R is denoted by $|R|$, I is an $n \times n$ identity matrix, R^{-1} is the inverse of correlation matrix, and the superscript T is the transpose sign.

2.2. Spatial Copula

Assume that there is a second-order stationary variable, Z, with distribution function, F_Z, sampled at some points, N. According to the second-order stationary condition, the following property can be seen for two sets of samples separated by a vector, $\boldsymbol{h}$:

$$P(Z(x_1) < v_1, \dots, Z(x_k) < v_k) = P(Z(x_1 + \boldsymbol{h}) < v_1, \dots, Z(x_k + \boldsymbol{h}) < v_k) \quad (8)$$

where, $v_1, \dots, v_k$ are some possible thresholds and $Z(x_1)$ denotes the value of Z at location x_1. Therefore, the empirical copula can be written as a function of distance as follows:

$$C_s(\boldsymbol{h}, u, u) = P\big(F_Z(Z(x)) < u, F_Z(Z(x + \boldsymbol{h})) < u\big) = C\left(F_Z(Z(x)), F_Z(Z(x + \boldsymbol{h}))\right) \quad (9)$$

Application of copulas in geostatistical estimations needs considering distance parameter in copula models. For multivariate Gaussian copulas, this procedure can be done by calculating auto/cross-correlograms. For our case, which is a bivariate representation of Gaussian copulas, calculation of auto-correlogram of Z at several lags and fitting it with an appropriate model provides a helpful tool.

By putting sample distances from the estimation point into the model correlogram function, conditional copula density for the estimation point can be calculated. By integrating the conditional density using any numerical method and standardizing it, the conditional distribution function for the estimation point can be obtained. This allows to calculate the mean value of variable at unknown location and its confidence interval at a significant level from the conditional distribution function. Please see Bardossy [12], Bardossy and Li [13], and Atalay and Tercan [15] for further reading on this subsection.

2.3. Steps of Estimation

Steps of estimation through spatial Gaussian copulas are as follows:

I) Transform variable into standard uniform distribution.

II) Calculate experimental auto/correlogram of the variable at several lags and fit them with an appropriate model.

III) Set the number of conditioning (NCD) samples used in estimation.

IV) Find conditional density function for the estimation point and find the conditional CDF through any numerical integration approach.

V) Find the median value (or mean value) and its confidence interval at a significant level to be back transformed into the data distribution.

2.4. Ordinary Kriging (OK)

OK is a well-known geostatistical technique for estimating an unknown value at un-sampled location. Theoretically, it is the best linear minimum variance estimator using variogram function characterizing the spatial variability. The OK assigns $\lambda_\alpha, \alpha = 1,2, \dots, n$ weights to the sample values to estimate variable of interest at the estimation node as follows [26]:

$$z^*(x_0) = \sum_{\alpha=1}^{n} \lambda_\alpha z(x_\alpha) \quad (10)$$

where n is the number of conditioning data and $z^*(x_0)$ is the OK estimate at point x_0. λ_α weights are calculated by solving the OK system of equations presented in the matrix form as follows:

$$\begin{bmatrix} \gamma_{11} & \gamma_{12} & \dots & \gamma_{1n} & 0 \\ \gamma_{21} & \gamma_{22} & \dots & \gamma_{2n} & 0 \\ \vdots & \vdots & \ddots & \vdots & \vdots \\ \gamma_{n1} & \gamma_{n2} & \dots & \gamma_{nn} & 0 \\ 0 & 0 & 0 & 0 & 1 \end{bmatrix} \begin{bmatrix} \lambda_1 \\ \lambda_2 \\ \vdots \\ \lambda_n \\ -\mu \end{bmatrix} = \begin{bmatrix} \gamma_{01} \\ \gamma_{02} \\ \vdots \\ \gamma_{0n} \\ 1 \end{bmatrix} \quad (11)$$

μ and γ_{ij} are respectively the Lagrange multiplier and the variogram between points i and j.

Calculation of confidence intervals is not an intrinsic property of the OK estimator; however, application of multi-Gaussianity assumption makes it possible to estimate symmetric confidence intervals, CI_{OK}, using the following formula:

$$CI_{OK} = z^*(x_0) \pm \varrho \times \sigma \quad (12)$$

where, σ is the standard deviation of the errors calculated from kriging variance and ϱ is the confidence level value.

2.5. Indicator Kriging (IK)

The IK belongs to non-linear estimation methods that basically allow to derive conditional cumulative distribution functions (CCDF) [27]. It is based on transforming raw data into indicator values as follows:

$$I(x_\alpha, v_i) = \begin{cases} 1, & if\ z(x_\alpha) \le v_i, i = 1, \dots, K \\ 0, & else \end{cases} \quad (13)$$

where K is the number of thresholds. Multiple IK requires to compute indicator variograms for each threshold and use them in the estimation of the CCDFs. The mean, median, and upper and lower bounds of confidence interval can be obtained from the CCDFs.

2.6. Performance criteria

Performance of the methods are first assessed by global accuracy and precision of the distribution of estimates. Global accuracy is defined as the fraction of estimated values falling within fixed symmetric probability intervals derived from data. A probability distribution is globally accurate if the fraction of true values falling inside the p interval exceeds p for all p in [0, 1] [28-30]. Global precision is a measure of the narrowness of the distribution and is only defined for accurate distributions. The precision of an accurate distribution is measured by the closeness of the fraction of estimated values to p for all p in [0, 1].

For globally accurate and precise estimates, summary statistics such as mean bias error (MBE), mean square error (MSE), degree of smoothing (measured by variance of the estimates) and conditional biasedness are considered for further assessment. A robust estimator has the lowest MBE, MSE, and conditional biasedness.

3. Case Study

The Sungun porphyry copper deposit, the second largest deposit of its type in Iran, is located 130 km north of Tabriz (**Figure 1**). It is one of the intrusive stocks that occur within the Urmia-Dokhtar magmatic arc. This NW-SE striking arc, which belongs to the Tertiary period, occurred due to the subduction of the Neo-Tethyan oceanic crust beneath the Iranian plate in late Mesozoic and early Cenozoic eras [31-32]. The NW part of this belt includes the Sungun deposit and is called the Ahar–Jolfa (Arasbaran) zone. This zone generally contains Cretaceous–Cenozoic volcanic and sedimentary units and Cenozoic plutonic igneous rocks.

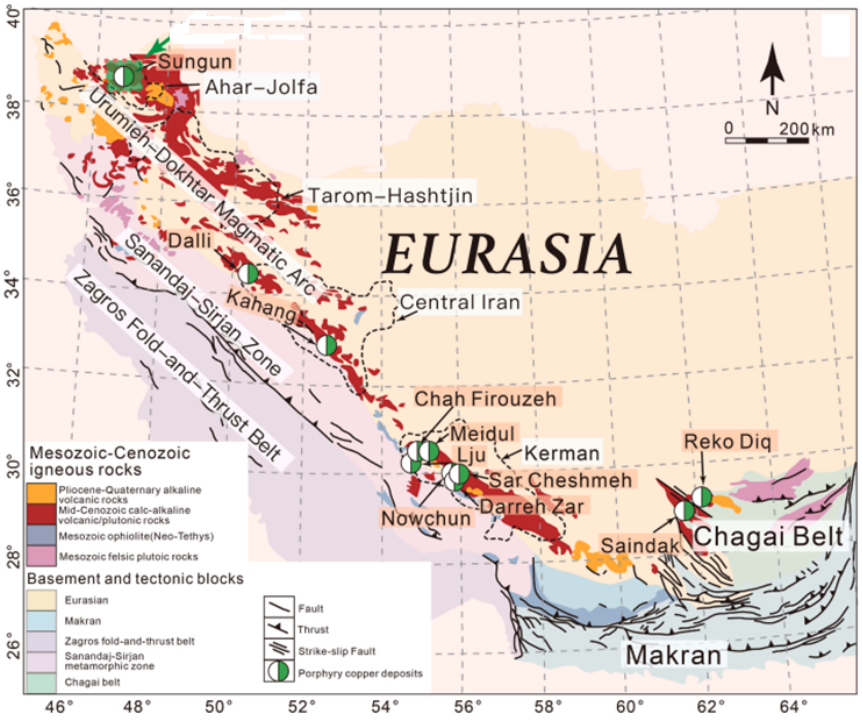

Figure 1. The Urumia–Dokhtar magmatic arc in map of Iran [33].

Monzonite/quartz-monzonite and later diorite/granodiorite are the major plutonic, igneous rocks in the west and east part of the region, respectively. Cretaceous limestone encompasses these bodies from north and east. The north and western parts of the deposit is characterized by the presence of andesitic to dacitic dykes. Ore bearing trachyandesitic dykes are common in the diorite/granodiorite unit and occur with less density in quartz-monzonite. A small Skarn-type formation occurs in the contact zone of the porphyritic monzonite and limestone in north-east edge of the stock [34-35] (**Figure 2**).

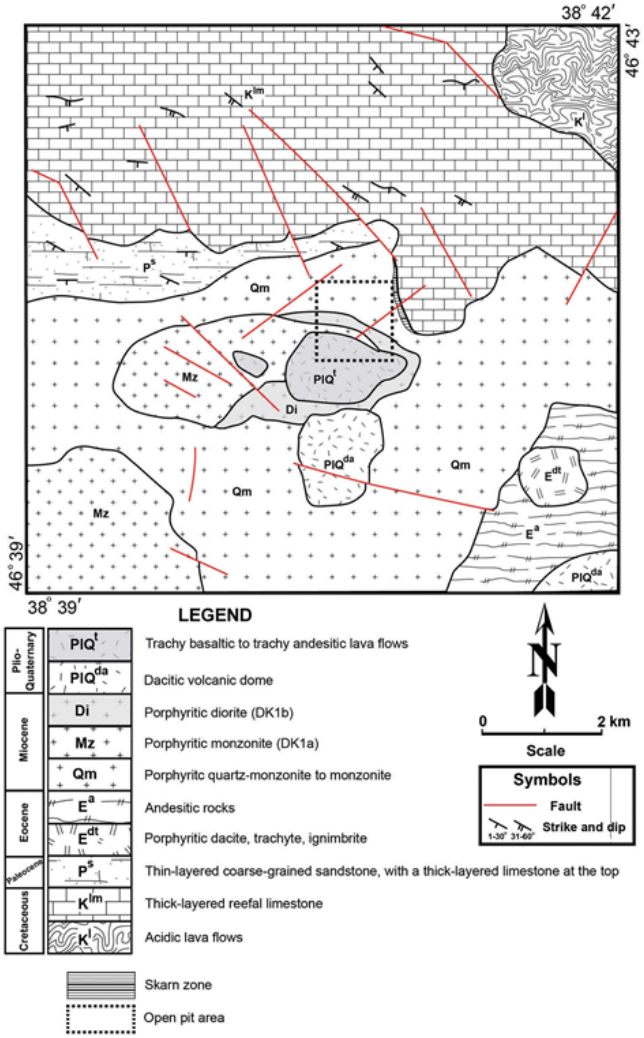

Figure 2. A geologic map of the Sungun deposit [36].

Intense shattering and hydro-fracturing can be seen in the central part of the quartz-monzonite porphyry stock caused by various types of cross-cutting vein-lets and micro-veinlets of quartz, quartz–sulfide, sulfides, sericite, carbonates and sulfates [37]. Ore-bearing hydrothermal fluids and sulfur with mainly magmatic origin have created extensive alteration zones and sulfide mineralization within the porphyry stock. These alteration zones namely potassic, phyllic, argillic, and propylitic can be seen from center to outside the stock [38]. Sulfide mineralization including hypogene pyrite, chalcopyrite and molybdenite has mainly occurred in the potassic and phyllic alteration zones. A thin sulfide-enriched supergene zone caused by weathering and leaching of the primary sulfide minerals covers the hypogene zone.

3.1. Data Description

Data used in this study come from core samples of 100 exploratory boreholes drilled in the western bank of the Pakhirchai river in the Sungun deposit and belong to Porphyry mineralization. Two-meter-long composites were created by

considering the average length of the core samples. Regarding geological information and statistical analysis of Cu concentrations, the deposit was laterally divided into phyllic (A) and potassic (B) alteration zones. Figure 3 presents a location map of the boreholes and Table 1 gives summary statistics of copper grades. Due to the lack of connectivity in the supergene zone and its limited number of samples, separate geostatistical evaluation of supergene mineralization would not be helpful. Therefore, vertical zoning was not considered and zones A and B include both hypogene and supergene mineralization.

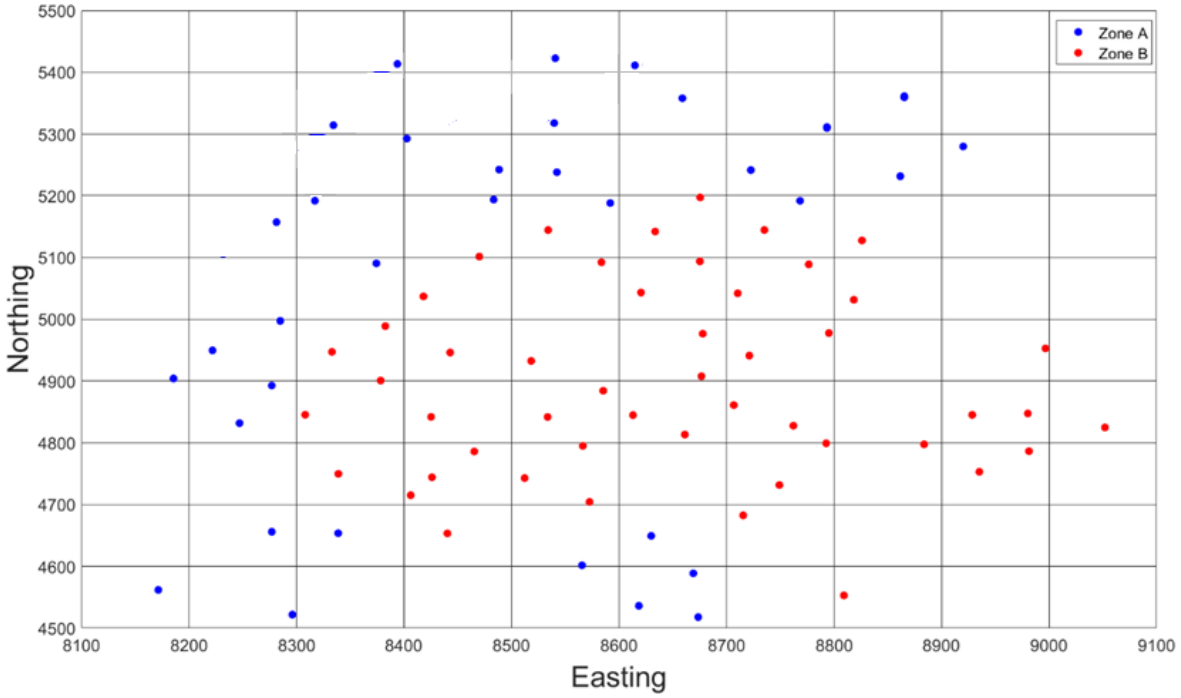

Figure 3. Location map of the boreholes. Blue and red dots stand for zones A and B.

Table 1. Summary statistics of the copper grade (%).

Zone	Sample size	Mean	Min	Max	Median	Skewness	Kurtosis	Variance
A	2311	0.417	0.020	1.420	0.354	1.133	1.051	0.080
B	3166	0.772	0.021	1.419	0.791	-0.127	-0.769	0.106

3.2. Spatial Variability Analysis

It should be mentioned that OK and IK were implemented in the Stanford Geostatistical Modeling Software (SGeMS) and GC was performed using a MATLAB code developed by the authors. Comparison among OK, GC, and IK was implemented running the Jackknife test of cross-validation by randomly dividing the composites of each zone into data and validation sets with statistical properties shown in Table 2. The data and validation sets have similar distributions with close mean values, skewness, and variances.

Table 2. Summary statistics for the data and validation sets.

Zone	Set	Sample size	mean	skewness	Kurtosis	Variance
A	data	2011	0.416	1.145	1.108	0.079
	Validation	300	0.422	1.054	0.733	0.084
B	data	2497	0.772	-0.167	-0.741	0.103
	Validation	669	0.772	-0.002	-0.870	0.116

Prior to estimation through OK, GC, and IK, the data sets were transformed into the Gaussian distribution, uniform distribution, and indicator data, respectively. Uniform transformation was directly performed based on experimental data by sorting them from the lowest to the largest values and putting their ranks as their new values. However, one could use different symmetric or

asymmetric kernel density estimators to estimate probability distribution function and apply it in the transformation. In our case using kernel density estimators did not have any positive impact on the results. The methods were implemented on the transformed data and the OK and GC results were back transformed into original space using the inverse functions. Indicator data sets were generated considering 11 thresholds that correspond to the 2.5th, 10th, 20th, 30th, 40th, 50th,60th, 70th, 80th, 90th and 97.5th percentiles of Cu grades.

The transformed data were analyzed to describe the spatial dependence structure of Cu for choosing parameters in the Jackknife test and for estimating the nodes of a 3D regular mesh ($12.5m \times 12.5m \times 12.5m$). For each zone, variograms of the normalized and indicator values were analyzed in downhole and horizontal directions. The experimental variograms of the normalized data showed no severe anisotropy so that the omnidirectional variograms were retained for modelling (Figure 4). The models consist of a nugget effect, a short-range exponential model, plus a long-range spherical model. Table 3 presents contribution and range for each structure. Note that Zone B shows higher short-range variability (larger nugget effect) and lower continuity (smaller range) than Zone A.

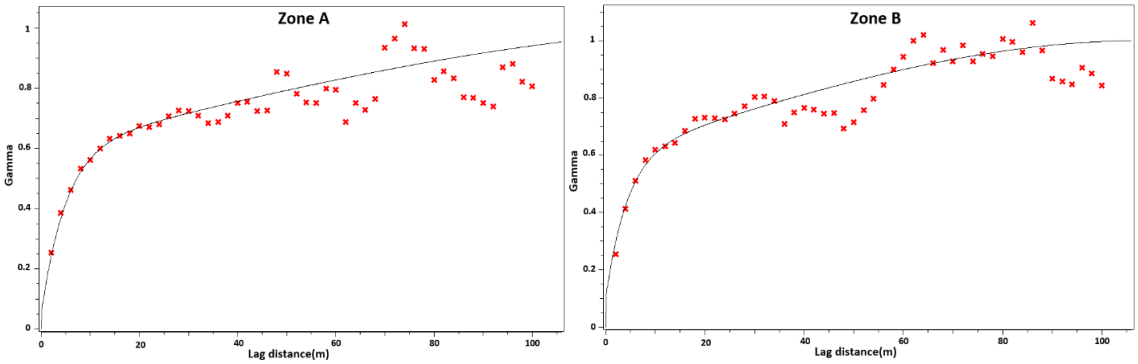

Figure 4. Omnidirectional variograms of the normalized Cu (crosses) and fitted models (black solid line).

Table 3. Model variogram parameters for the normalized data.

	Nugget	Structure #1	Contribution 1	Range 1(m)	Structure #2	Contribution 2	Range 2(m)
Zone A	0.05	Exponential	0.55	15	Spherical	0.40	150
Zone B	0.1	Exponential	0.50	13	Spherical	0.40	108

Variography of indicator sets showed geometric anisotropy with short ranges in downhole direction. These variograms (not shown here due to their large numbers) demonstrated nested structures that consist of a nugget effect, a short-range exponential model, and a long-range spherical model.

For estimation through GC, omnidirectional correlograms of the uniform data were calculated (Figure 5) and fitted by suitable models with parameters presented in Table 4. Consistent with the normalized variograms, the correlogram of Zone B shows lower correlation at short distances and lower range than Zone A.

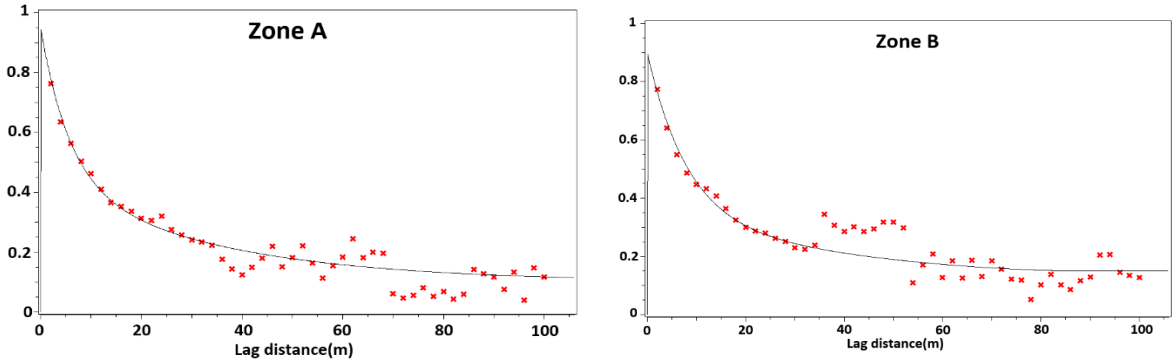

Figure 5. Correlograms (crosses) of the uniform data for zones A and B and fitted models (black solid line).

Table 4. Model correlogram parameters used in copula estimations.

	Nugget	Structure #1	Contribution 1	Range 1(m)	Structure #2	Contribution 2	Range 2(m)
Zone A	0.95	Exponential	-0.50	17	Exponential	-0.35	100
Zone B	0.90	Exponential	-0.60	25	Spherical	-0.15	90

3.3. Performance Assessment by Running a Jackknife Test

Performance assessment of the methods was implemented by running a Jackknife test and comparing the estimates to the observed values.

Estimation through GC, IK, and OK methods was implemented choosing exactly 17 conditioning data. Seventeen conditioning data were chosen after trying different values by evaluating the cross-validation results of the three methods. Increase in the number of conditioning data (NCD) would result in better estimation of the mean value; however, it would negatively increase the smoothing problem. Note that the estimation results of the three methods were proportionally affected from the NCD. Search neighborhood of OK and IK was considered large enough to encompass 17 samples. Advanced search options such as octant search were not used in the selection of conditioning data. In IK, the CCDFs were generated considering linear relationships between the lower class and minimum data value and upper class and maximum data value with no extrapolation. In IK and GC methods, the e-type values of CCDFs were assigned as the estimated value.

For global accuracy and precision assessment of the distribution of the estimates produced by the three methods the symmetric p_i-probability intervals with $p_i = 0.1 \times i, i = 1,2,\dots,9$ were built by using the actual data and computing the fraction of the estimated values falling inside the corresponding intervals. Figure 6 shows the plot of actual coverage against the estimated coverage for both zones.

Figure 6 shows that the GC and IK estimates are accurate in both zones because they produce estimated p values exceeding actual p values. OK is globally accurate in zone A but not in zone B.

Inaccuracy of the OK estimates in zone B results from the first two points that are slightly below the1:1 line. In zone A, the OK results have the highest degree of precision and the GC estimates come in the second place while IK has the worst performance in precision. Since global precision matters only for accurate estimates, assessing the precision of OK estimates in zone B does not make sense. Global precision test shows advantage of GC over IK due to its estimated p values that are close to the line of equality.

In the second step of performance analysis, the summary statistics of the estimates are compared to that of the data. Table 5 presents the cross-validation results of the three methods for both cases. IK has the lowest absolute MBE and MSE, followed by GC and OK. The superiority of IK over GC and OK can be misleading without considering conditional biasedness and variability of the estimates.

Table 5. Cross-validation results for OK, GC and IK methods.

Zone	Method*	MBE**	MSE***	Variance
A	OK	-0.104	0.084	0.030
	GC	-0.089	0.084	0.027
	IK	-0.044	0.066	0.014
B	OK	-0.173	0.183	0.066
	GC	-0.124	0.149	0.050
	IK	-0.073	0.125	0.014

*For a fair comparison the number of conditioning data is chosen to be 17 for all methods

Figures 7 and 8 present the Q-Q plots of the estimated values versus real observations and the box plots constructed to examine the conditional biasedness and variability. Note that IK has a serious smoothing problem, and it produces nearly the similar grade estimates around the mean value of data. For example, IK estimates change around and at 0.38 Cu% in 0.4-0.8 Cu% range of the actual data in zone A and 0.65 Cu% in 0.4-1.2 Cu% range in zone B. The same observations can also be made for the box plots (Figure 8). The smoothing property of IK estimates is consistent with the literature [39-40].

From Table 5 and Figures 7 and 8, it is clear that OK produces the estimates with the highest variability. On the other hand, the estimates of OK are systematically lower, especially in zone B. This

bias has resulted in weak accuracy of OK in zone A and inaccurate estimates in zone B.

Better performance of OK in zone A relative to zone B can be related to smaller nugget effect of the Cu variograms in this zone. The decreasing efficiency of OK with increasing nugget effect is also observed in Sohrabian [41-42].

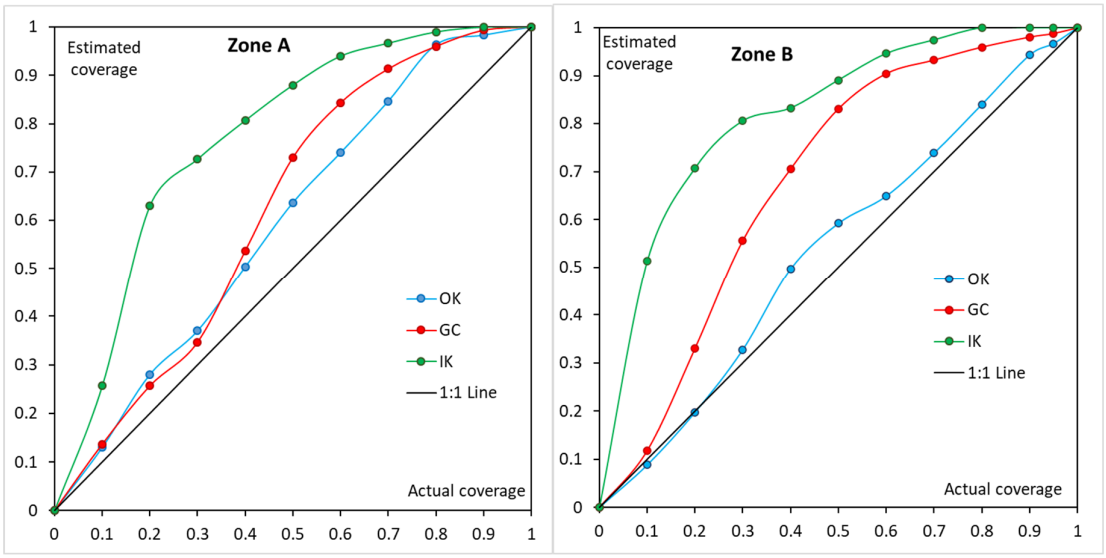

Figure 6. Global accuracy and precision test of the estimates.

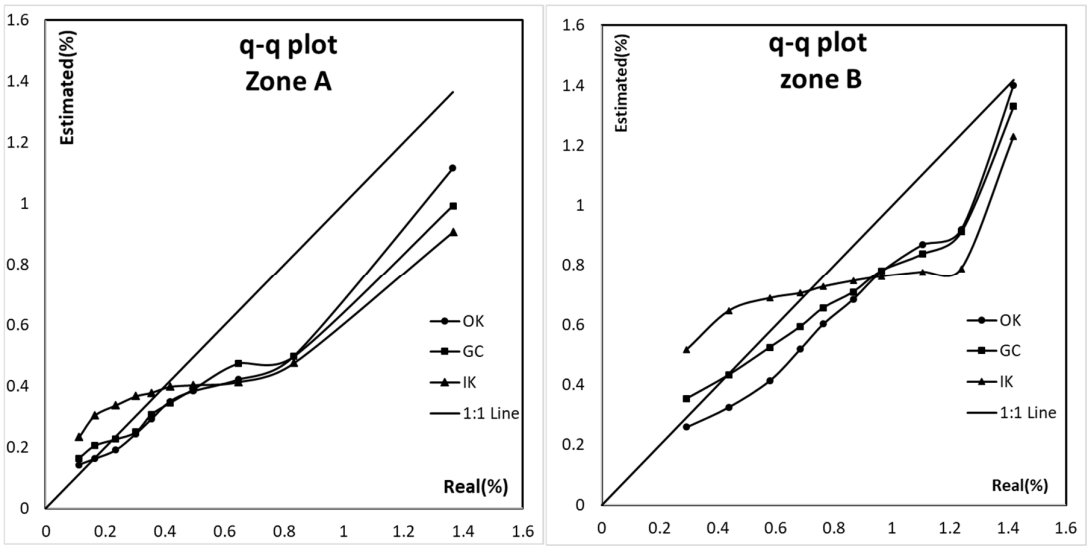

Figure 7. Q-Q plots of the estimates versus the real values.

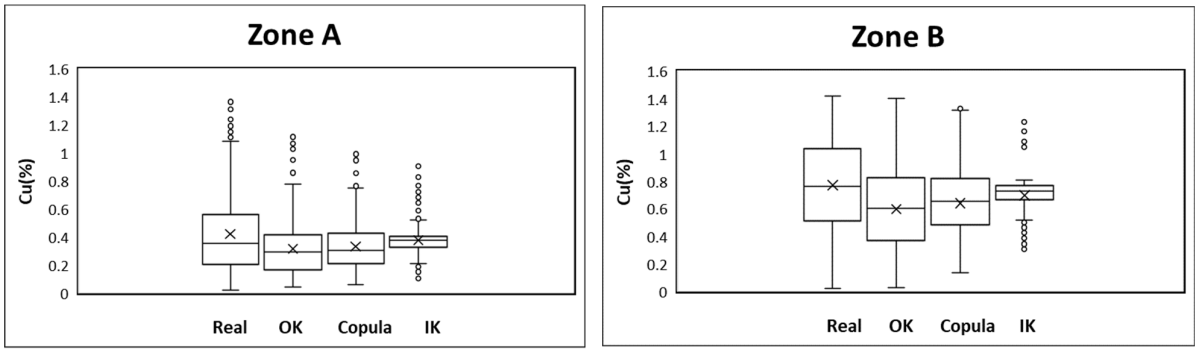

Figure 8. Box plots of the estimates.

3.4. Grade Estimation in the Copper Deposit

Grade estimation was made at the grid nodes of a 3D mesh with sizes 12.5m×12.5m×12.5m in each zone separately by using the three methods. The total number of points estimated is 82,268. The copula, variogram, and indicator variogram parameters obtained from the Jackknife test were considered in the estimation. Figure 9 shows the spatial distributions of the estimates for zone A and zone B. It is evident that IK produces very smooth estimates and practically GC and OK estimates show similar spatial distributions.

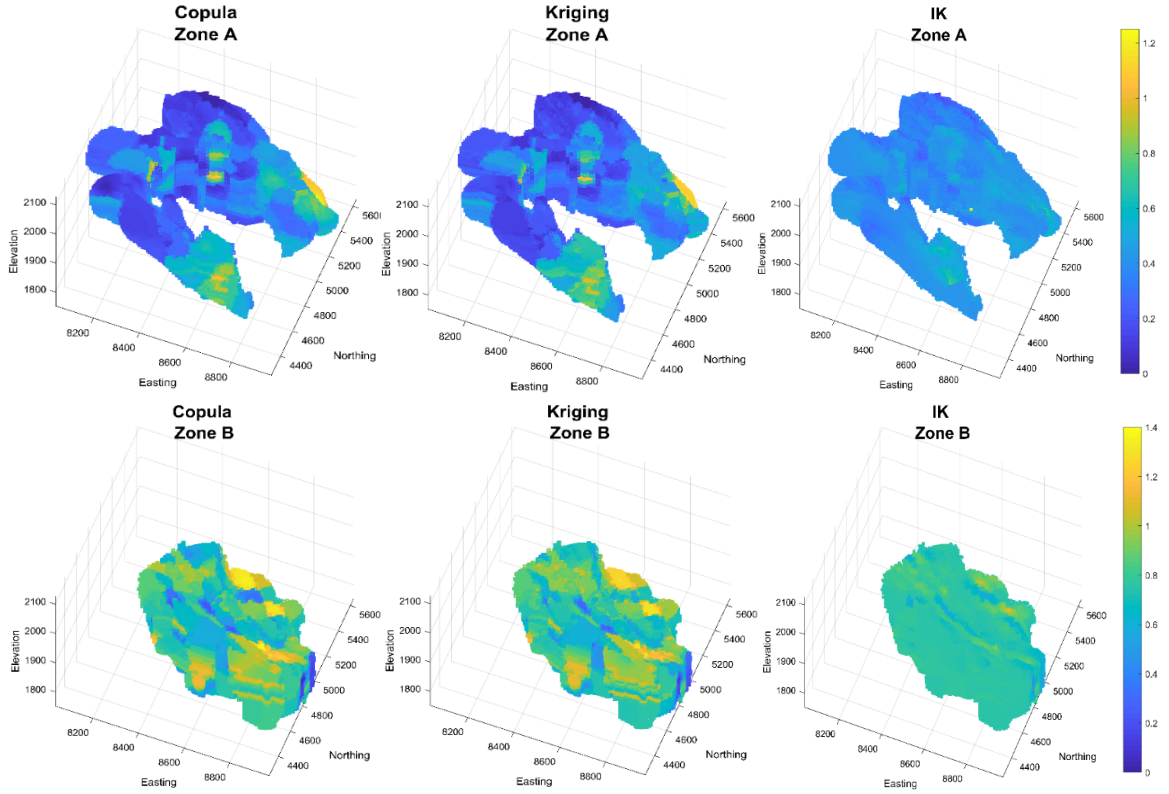

Figure 9. 3D maps of the estimated blocks.

4. Conclusions

This study compares three estimation methods, GC, OK and IK, using a case study in the Sungun copper deposit. GC and IK are basically methods that allow to derive the conditional cumulative distribution functions and any type of estimates in GC and IK are obtained from the cumulative distribution while OK directly estimates unknown values at un-sampled locations.

In terms of global distribution of the estimates, OK can provide globally inaccurate estimates, IK gives accurate but imprecise estimates while GC produces both globally accurate and precise estimates.

Cross validation study shows that OK results have high variability but less confidence due to high errors. IK generates significantly smooth values with the lowest errors because the estimated values are gathered around the mean. However, having the lowest MBE and MSE does not make sense. The GC estimates are generally reasonable in terms of MBE, MSE and variability. The grade estimation made in the copper deposit supports the smoothing property of the IK estimates and shows similar grade patterns for GC and OK.

The case study proves that GC has advantages over OK and IK since it is a globally accurate and precise estimator and produces acceptable error statistics and variability.

Acknowledgment

"This publication has been produced benefiting from the 2236 Co-Funded Brain Circulation Scheme2 (CoCirculation2) of TÜBİTAK (Project No: 121C369). However, the entire responsibility of the publication belongs to the owner of the publication. The financial support received from TÜBİTAK does not mean that the content of the publication is approved in a scientific sense by TÜBİTAK."

References

[1]. Bastante, F.G., Taboada, J., Alejano, L.R., & Ordóñez, C. (2005). Evaluation of the resources of a slate deposit using indicator kriging. *Engineering Geology*, *81(4)*, 407-418.

[2]. Heriawan, M.N., & Koike, K. (2008). Uncertainty assessment of coal tonnage by spatial modeling of seam distribution and coal quality. *International Journal of Coal Geology*, *76(3)*, 217-226.

[3]. Vargas-Guzmán, J. (2008). Unbiased Resource Evaluations with Kriging and Stochastic Models of Heterogeneous Rock Properties. *Nat Resour Res*, *17*, 245–254.

[4]. Daya, A.A. (2012). Reserve estimation of central part of Choghart north anomaly iron ore deposit through ordinary kriging method. *International Journal of Mining Science and Technology*, *22(4)*, 573-577.

[5]. Moosavi, E., & Gholamnejad, J. (2015). Long-term production scheduling modeling for the open pit mines considering tonnage uncertainty via indicator kriging. *J Min Sci*, *51*, 1226–1234.

[6]. Monteiro da Rocha, M., & Yamamoto J.K. (2000). Comparison between kriging variance and interpolation variance as uncertainty measurements in the Capanema Iron Mine, State of Minas Gerais-Brazil. *Nat Resour Res*, *9*,223–235.

[7]. Lloyd, C., & Atkinson, P. (2001). Assessing uncertainty in estimates with ordinary and indicator kriging. *Computational Geosciences*, *27(8)*, 929–937.

[8]. Carr, J., & Mao, N. (1993). A general-form of probability kriging for estimation of the indicator and uniform transforms. *Math* Geol,*25(4)*, 425–438.

[9]. Carle, S., & Fogg, G. (1996). Transition probability-based indicator geostatistics. *Math Geol, 28(4)*, 453–476.

[10]. Bogaert, P. (1999). On the optimal estimation of the cumulative distribution function in presence of spatial dependence. *Math Geol,3(2)*, 213–239.

[11]. Pardo-Igúzquiza, E., & Dowd, P. (2005). Multiple indicator cokriging with application to optimal sampling for environmental monitoring. *Computational Geoscience, 31(1)*,1–13.

[12]. Bardossy, A. (2006). Copula-based geostatistical models for groundwater quality parameters. Water Resour. Res, 42.

[13]. Bardossy, A., & Li, J. (2008). Geostatistical interpolation using copulas. *Water Resour. Res, 44*.

[14]. Kazianka, H., & Pilz, J. (2010). Copula-based geostatistical modeling of continuous and discrete data including covariates. *Stoch. Env. Res. Risk A., 24,* 661–673.

[15]. Atalay, F., & Tercan, A.E. (2017). Coal resource estimation using Gaussian copula, *International Journal of Coal Geology, 175*.

[16]. Käärik, E., & Käärik, M. (2009). Modeling dropouts by conditional distribution, a copula-based approach. *Journal of Statistical Planning and Inference, 139(11)*, 3830-3835.

[17]. Parsa, R.A., & Klugman, S.A. (2011). Copula regression. *Var. Adv. Sci. Risk, 5*, 45-54.

[18]. Kwak, M. (2017). Estimation and inference on the joint conditional distribution for bivariate longitudinal data using Gaussian copula, *Journal of the Korean Statistical Society, 46(3)*, 349-364.

[19]. Chang, B., & Joe, H. (2019). Prediction based on conditional distributions of vine copulas, *Computational Statistics & Data Analysis, 139*, 45-63.

[20]. Musafer, G. N., Thompson, M. H., Kozan, E., & Wolff, R. C. (2016). Spatial Pair-Copula Modeling of Grade in Ore Bodies: A Case Study. *Natural Resources Research, 26(2)*, 223–236.

[21]. Addo, E., Chanda, E.K., & Metcalfe, A.V. (2017). Estimation of direction of increase of gold mineralization using pair-copulas, *International Congress on Modelling and Simulation*.

[22]. Sohrabian, B., Soltani-Mohammadi, S., Pourmirzaee, R., & Carranza, E.J.M. (2023). Geostatistical Evaluation of a Porphyry Copper Deposit Using Copulas. *Minerals, 13(6)*, 732.

[23]. Bárdossy, A., & Hörning, S. (2023). Definition of Spatial Copula Based Dependence Using a Family of Non-Gaussian Spatial Random Fields. *Water Resources Research, 59(7)*.

[24]. Sklar, A. (1959). Fonctions de Répartition à n Dimensions et Leurs Marges. *Publications de l'Institut Statistique de l'Université de Paris, 8*, 229-231.

[25]. Addo, E., Chanda, E.K. & Metcalfe, A.V. (2018). Spatial Pair-Copula Model of Grade for an Anisotropic Gold Deposit. *Mathematical Geosciences, 51(5)*, 553–578.

[26]. Isaaks, E.H., & Srivastava, R.M. (1989). An Introduction to Applied Geostatistics. *Oxford University Press, New York, 413*.

[27]. Journel, A.G. (1983). Nonparametric estimation of spatial distributions. *Math. Geol., 15*, 445–468.

[28]. Tercan, A.E., & Dowd, P.A. (1995). Approximate Local Confidence Intervals under Change of Support. *Mathematical Geology, 27(1)*, 149–72.

[29]. Deutsch, C.V. (1996). Direct Assessment of Local Accuracy and Precision. *Geostatistics Wollongong 96, Vol 1, Baafi and Schofield, editors, Kluwer Academic Publishers*, pp 115-125.

[30]. Pyrcz, M.J., & Deutsch, C.V. (2014). Geostatistical Reservoir Modeling, 2nd Edition, *Oxford University Press, New York*, p. 448.

[31]. Berberian, M., & King, G.C.P. (1981). Towards a paleogeography and tectonic evolution of Iran, *Canadian Journal of Earth Sciences, 18*, 210–265.

[32]. Alavi, M. (1991). Sedimentary and structural characteristics of the Paleo-Tethys remnants in northeastern Iran, *Geological Society of America Bulletin, 103*, 983–992.

[33]. Kou, G.Y., Xu, B., Zhou, Y., Zheng, Y.C., Hou, Z.Q., Zhou, L.M., Zhang, L.M., & Yu, J.X. (2021). Geology and petrogenesis of the Sungun deposits: Implications for the genesis of porphyry-type mineralisation in the NW Urumieh–Dokhtar magmatic Arc, Iran. *Ore Geology Reviews [Internet]*.

[34]. Lescuyer, J.L., Riou, R., Babakhani, A., Alavi Tehrani, N., Nogol, M.A., Dido, J., & Gemain, Y.M. (1978). Geological map of the Ahar area. *Geological Survey of Iran*.

[35]. Mehrpartou, M. (1993). Contributions to the geology, geochemistry, ore genesis and fluid inclusion investigations on Sungun Cu–Mo porphyry deposit, (North-West of Iran). *PhD Thesis, Hamburg University 1993. Hamburg*, 245 pp.

[36]. Simmonds, V., Moazzen, M., & Mathur, R. (2017). Constraining the timing of porphyry mineralization in northwest Iran in relation to Lesser Caucasus and Central Iran; Re–Os age data for Sungun porphyry Cu–Mo deposit. *International Geology Review, 59(12)*, 1561–1574.

[37]. Calagari, A.A., Pattrick, R.A.D., & Polya, D.A. (2001). Veinlets and micro-veinlets studies in Sungun porphyry copper deposit, East Azarbaidjan, Iran. *Iranian Journal of Geoscience, 39–40*, 70–79.

[38]. Soltani, F., Afzal, P., & Asghari, O. (2014). Delineation of Alteration Zones Based on Sequential Gaussian Simulation and Concentration–Volume Fractal Modeling in the Hypogene Zone of Sungun Copper Deposit, NW Iran. *Journal of Geochemical Exploration, 140*, 64–76.

[39]. Sullivan, J. (1984). Non-parametric estimation of spatial distributions. *Unpublished PhD dissertation, Stanford University*, 367 pp.

[40]. Myers, J.C. (1997). Geostatistical Error Management: Quantifying Uncertainty for Environmental Sampling and Mapping, *John Wiley and Sons*, 596 pp.

[41]. Sohrabian, B. (2021a). Geostatistical prediction through convex combination of Archimedean copulas. *Spatial Statistics, 41*, 100488.

[42]. Sohrabian, B. (2021b). Capacity assessment of Gumbel-Clayton copula for geostatistical estimation. *Iran J Min Eng, 16(51)*, 52–67.

تخمین عیار با استفاده از کاپیولای گوسی: مطالعه موردی

بابک سهرابیان[1*] و عبدالله ارهان ترجان[2]

۱- گروه مهندسی معدن، دانشکده محیط زیست،دانشگاه صنعتی ارومیه، ارومیه،ایران

۲- گروه مهندسی معدن، دانشگاه حاجت تپه، آنکارا،ترکیه

ارسال ۲۰۲۴/۰۳/۰۵، پذیرش ۲۰۲۴/۰۶/۲۸

* نویسنده مسئول مکاتبات: babak_sohrabian@uut.ac.ir

چکیده:

منابع معدنی معمولاً از طریق روش کریجینگ که وزن نمونه ها را بر اساس فاصله واریوگرام تا نقطه برآورد بدون در نظر گرفتن مقادیر آنها تعیین می کند، تخمین زده می شود. تخمینگرهای قوی‌تر مانند کاپیولاهای فضایی ابزارهای امیدوارکننده‌ای است، زیرا آنها هم فاصله و هم مقادیر نمونه را در تعیین وزن‌ها در نظر می‌گیرد.هدف از این مطالعه نشان دادن اثربخشی کاپیولا های گاوسی از طریق تخمین مقدار عیار مس در کانسار مس پورفیری سونگون واقع در ایران است. عملکرد این روش با روش های کریجینگ معمولی و کریجینگ شاخص از طریق اجرای آزمون اعتبارسنجی متقابل جک نایف مقایسه شده است. معیارهای مورد استفاده در بررسی عملکرد این روش‌ها، صحت و دقت در توزیع مقادیر تخمین زده شده، آمار خطا و میزان تغییرپذیری در برآوردهای دارای صحت و دقت سراسری است. مطالعه موردی، مزیت های کاپیولای گوسی را نسبت به کریجینگ معمولی و کریجینگ شاخص نشان می دهد، بطوریکه نتایج تخمین زده شده توسط کاپیولا دارای صحت و دقت سرتاسری و تغییرات قابل قبول است و آمار خطای مناسبی دارد.

کلمات کلیدی: کاپیولای گوسی، کریجینگ شاخص، تست جک نایف، کریجینگ معمولی، نهشته مس پورفیری.